

S. WISSEL   
G. GRÜNEFELD

# Flow-field measurements of liquid and gaseous phases in the ultra-dense region of diesel sprays

Lehr- und Forschungsgebiet Laser-Messverfahren in der Thermofluidodynamik,  
Schinkelstraße 8, 52062 Aachen, Germany

Received: 8 February 2006/Revised version: 28 February 2006

Published online: 30 March 2006 • © Springer-Verlag 2006

**ABSTRACT** The velocities of both the liquid and the gaseous phases in a diesel spray are determined for the first time simultaneously via laser flow tagging (LFT). The experimental setup and uncertainties introduced by seeding particles in the gas phase are greatly reduced by using phosphorescent tracer molecules, i.e. acetone and biacetyl, for the gaseous phase. In addition, simultaneous droplet velocimetry is achieved by doping the liquid fuel with a lanthanide–chelate complex. The relative velocity of gas and liquid phases can be determined from the data on the spray axis close to the nozzle for the first time. This is an important quantity for modeling droplet break-up and evaporation in ultra-dense sprays.

PACS 42.62.-b; 47.61.Jd

## 1 Introduction

The experimental analysis of diesel fuel injection and dense sprays in general is of major economic and ecological importance, since fuel sprays are used for a large fraction of the global energy consumption. Besides the support of engine research and development by numerical simulations of the entire injection, evaporation and combustion processes, experimental work is necessary in order to provide precise data for validation of spray models. Particularly, the droplet and gaseous-phase velocities inside dense sprays are rare but vital information, since the relative velocity is one important parameter regarding droplet break-up and evaporation processes.

However, most commonly used laser diagnostics fail in the application in very dense sprays, mostly due to the high number density of droplets, introducing severe multiple scattering of the incident and emitted light. Furthermore, most methods for velocity deter-

mination rely either on the detection of single particles or droplets, e.g. phase Doppler anemometry (PDA) [1], or the imaging of an ensemble of droplets, like particle image velocimetry (PIV) [2]. While the aforementioned techniques suffer from the necessity of seeding particles and the uncertainties introduced by particle inertia, other techniques such as laser correlation velocimetry (LCV) and its derivatives [3, 4] are bound to atmospheric or low-pressure conditions.


To overcome the problems of seeding particles, a variety of so-called flow tagging techniques has been developed, which use either photochemical or photophysical effects of molecular tracers for velocimetry as follows. A unique structure in the flow is created ('write' process), whose displacement  $\Delta s$  is subsequently tracked ('read' process). With the delay  $\Delta t$  between the 'writing' and 'reading' processes the velocity  $v$  can be determined via  $v = \Delta s / \Delta t$ . Compared to the photochemical processes like dissociation [5, 6] or photophysical methods

such as ionization [7], the advantages of phosphorescence [8] are numerous. The long-lasting luminescence is excited by one UV-laser pulse and can afterwards be detected within its lifetime, thus simplifying the experimental setup and featuring comfortable means for acceleration measurements [9–11]. While several phosphorescent substances are available as soluble tracers for liquid fluids [11], only ketones such as acetone and biacetyl yielding phosphorescence lifetimes in the microsecond range are suitable for the application in the gas phase [8, 12, 13].

In this study a novel application of acetone as a phosphorescent tracer for flow-field measurements inside a diesel spray is presented. In addition, a molecular tracer in the model fuel enables the simultaneous determination of liquid and gaseous phase velocities, i.e. the relative velocity of the droplets or liquid ligaments.

## 2 Experimental

Simultaneous measurement of the displacement of the droplets and the entrained gas phase is achieved by non-interfering emissions from both phases. As shown in Fig. 1, the phosphorescence of acetone (seeded in the gas phase) and the europium ion (embedded in the lanthanide–chelate complex  $\text{Eu}:(\text{FOD})_3$ , which is dissolved in the fuel) can be separated by optical filters, see below. Spectral overlap of the acetone emission into the transmission range of the long-pass filter ( $\text{OG590} \times 3 \text{ mm}$ , Schott), which is used for the liquid phase, can be neglected due to the lower density of molecules in the gaseous phase and the weak inten-

 Fax: +49-241-8092927, E-mail: wissel@ltd.rwth-aachen.de

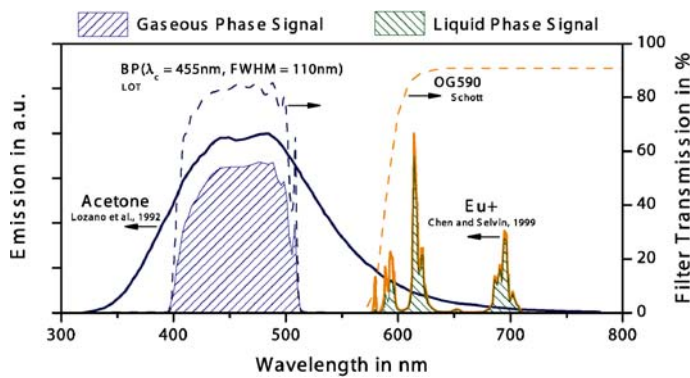


**FIGURE 1** Emission spectra of the tracers and filter transmission for spectral separation of liquid- and gas-phase signals; the emission of acetone corresponds to a  $3000\text{ cm}^{-1}$  shift compared to the fluorescence spectrum [15, 18]; the emission of the europium ion  $\text{Eu}^{3+}$  is according to [19]

sity of acetone phosphorescence. Vice versa, the band-pass filter (centered at 455 nm, FWHM = 110 nm, LOT-Oriel) efficiently blocks the emission bands of the europium ion with OD4.0.

The optical setup for the simultaneous measurements is illustrated in Fig. 2. A set of two prisms (wedge of approximately  $11^\circ$ , size  $50 \times 25\text{ mm}^2$ , fused silica) equipped with the filters mentioned above and a UV lens ( $f = 100\text{ mm}$ ,  $f_\# = 2.0$ , Halle) are used to image the emission of liquid- and gas-phase tracers onto one image-intensified double-frame camera (Nanostar S20, LaVision). For excitation, the beam of a XeCl-excimer laser (EMG 200, Lambda Physik) at 308 nm is split into several parallel beams with a distance of about 4 mm by an array of cylindrical lenses ( $f = 300\text{ mm}$ ). Velocities are evaluated by determination of the positions of the tag lines at  $t_0$  and  $t$  by fitting Lorentzian peak functions to intensity profiles parallel to the spray axis. The dynamic range seen in these particular

images is a factor of about 10. This does not represent the principal limit of the LFT technique.

Since phosphorescence of acetone and biacetyl is efficiently quenched by oxygen, the high-pressure vessel is filled with pure nitrogen. Furthermore, both tracer liquids are degassed to reduce the influence of oxygen quenching on the phosphorescence lifetime  $\tau$ . The triplet-state lifetimes observed in the experiments with excitation at 308 nm show significant deviation from the data found in the literature ( $13\ \mu\text{s}$  phosphorescence lifetime for acetone [13] and about 1.5 ms for biacetyl [14, 15]). This may be explained by insufficient gas exchange and yet remaining oxygen inside the vessel. The limited lifetime of the tracer emission restricts the accuracy of measurement and the application of this type of LFT to high-speed flows. However, the high-pressure automotive diesel sprays with droplet velocities of more than 100 m/s [4, 16] offer suitable conditions for this application. Due

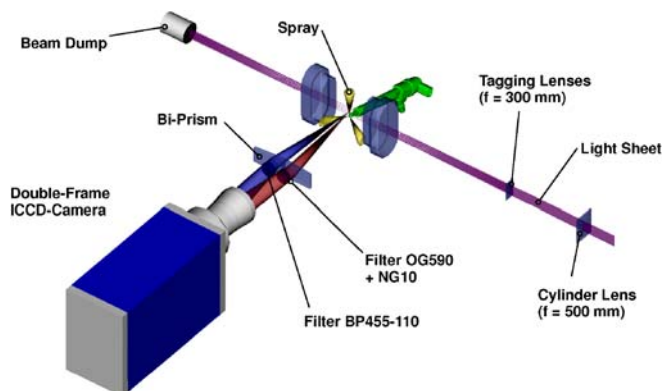


**FIGURE 2** Experimental setup of LFT for simultaneous velocimetry under high-pressure conditions (only the quartz windows of the pressure vessel are shown)

to its longer phosphorescence lifetime, biacetyl is the favorable tracer concerning the accuracy of measurement, which generally improves with increasing tag-line displacement. The simultaneous imaging in two-phase flows requires spectral separation of the emission of both tracers. Thus, acetone is chosen as gas-phase tracer in combination with  $\text{Eu}:(\text{FOD})_3$  for the liquid fuel in this application. For homogeneous seeding of the gas phase, a constant nitrogen flow (grade 4.0, Praxair) bubbles through a reservoir filled with acetone (GC > 99.9%, Merck Eurolab) or biacetyl (GC > 99.0%, Fluka) yielding an almost saturated atmosphere of about 25% acetone and 5% biacetyl by volume. The reservoir is installed as a by-pass in the supply system of the atmospheric vessel or the high-pressure chamber. Thus, the actual tracer concentration can easily be adjusted. The liquid-phase tracer europium tris(6,6,7,7,8,8,8-heptafluoro-2,2-dimethyl-3,5-octanedionate) ( $\text{Eu}:(\text{FOD})_3$ , Fluka) is dissolved in the model fuel *n*-dodecane (GC > 99%, Merck Eurolab) with a molar concentration of  $10^{-3}\text{ M}$ .

### 3 Results

Figure 3 shows typical results for the velocities in the gas phase (seeded with biacetyl) at three positions inside the spray for the injection under ambient conditions. It is the result of evaluating an averaged image of 20 single shots. The timing of measurement after energizing the injector  $t_{\text{aei}}$  is 0.4 ms with an injection duration  $\Delta t_{\text{id}}$  of 1.0 ms. The position is given as the distance  $H$  from the single excitation line to the nozzle tip. The background shows the averaged phosphorescence signal 1  $\mu\text{s}$  after laser excitation.  $\sigma_v/v$  is the relative error of each vector, which basically depends on the spatial displacement  $\Delta s$  and the signal-to-noise ratio SNR of the detected excitation line. The nozzle is a single-hole nozzle (sack hole) with a bore diameter of 230  $\mu\text{m}$ .

With increasing distance of the nozzle tip, the gas velocity increases from 107 m/s to 139 m/s on the spray axis, where the highest velocities are observed. Furthermore, the radial velocity profile is expanding whereas the velocity gradient at the spray edge de-

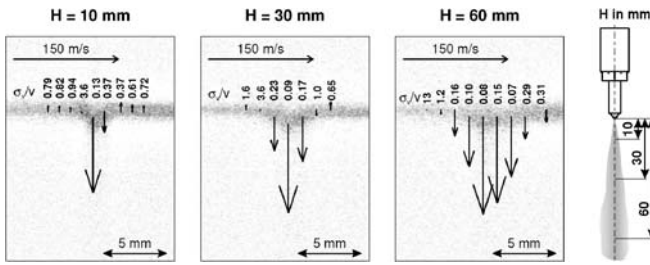


**FIGURE 3** Gas-phase velocity under ambient conditions at 300 bar rail pressure and biacetyl as tracer at different positions  $H$  from evaluation of averaged image (average of 20 pulses);  $t_{aei} = 0.4$  ms,  $\Delta t_{fid} = 1.0$  ms; background shows raw images of a single tagging line  $1 \mu\text{s}$  after laser excitation

creases. Close to the nozzle at the positions of 10 mm and 30 mm, fuel injection generates a weak recirculation area in the surrounding gas, as the results show a slight displacement in the opposite direction close to the spray cone. Though the measuring error is substantial with values between 37% and 160% here, the formation of a recirculation zone is reported in the literature, too [16, 17]. Apart from the significant error for the low velocities of less than 10 m/s in the surrounding gas phase, the relative error is in the range of 8% and

13% for the most interesting velocities on the spray axis.

The results from the simultaneous detection of liquid-phase ( $\text{Eu}:(\text{FOD})_3$ ) and gas-phase (acetone) signals under ambient conditions are shown in Fig. 4 for 300 bar and 500 bar injection pressures at 0.7 ms after start of injection. The nozzle is the same as in Fig. 3.

The highest droplet velocities 2 mm underneath the nozzle tip are 181 m/s and 320 m/s, respectively. While for an injection pressure of 300 bar the droplet velocity distribution is almost uniform

along the center line of the spray, momentum exchange with the gas phase causes significant deceleration of the droplets at the higher rail pressure of 500 bar. Here, the liquid-phase velocity on the spray axis decreases by 60 m/s within 60 mm. The relative error of the droplet velocity is about 2% on the center line, increasing slightly to 11% at the spray edge. Similar accuracy is achieved for the case of 300 bar rail pressure with a maximum uncertainty of 8%.

In agreement with [17], the gas-phase velocity is increasing with increasing distance from the nozzle tip. An exception is the case of 500 bar on the center line at 60 mm, where the velocity is about 10 m/s lower than at the corresponding position 30 mm further upstream with a velocity of 80 m/s. At higher injection pressure, the increased atomization of droplets amplifies the effect of multiple light scattering and results in broader tag lines. With a radial velocity distribution similar to those depicted in Figs. 3 and 4, the signal averaging over the increased line width tends to result in a lower velocity, since the slower areas in the outer region of the spray are included and are more pronounced.

The radial expansion of the gas, which is affected by the droplets, increases as the liquid spray cone widens. At 300 bar rail pressure the width increases from 1 mm close to the nozzle to about 10 mm at the distance of 60 mm (Fig. 4). This is about 40% larger than the liquid spray cone, which is corroborated by [17] and the results in Fig. 4b. The gas-phase velocity is determined with the lowest error on the spray axis at 60 mm of 10% and 20% for 300 bar and 500 bar, respectively. The accuracy deteriorates with both decreasing distance to the nozzle and further outward towards the more dilute region at the edge of the spray.

Finally, the first application of simultaneous LFT in the liquid and the gaseous phases under an elevated pressure of 5 bar is shown in Fig. 5. Results are given for two rail pressure conditions, i.e. pressure differences between fuel rail and gas pressure  $\Delta p_{\text{Rail-Chamber}}$  of 400 bar (left-hand side) and 800 bar (right-hand side). According to Bernoulli's condition for inviscid flows, the injection pressure results in a maximum droplet velocity of 327 m/s and

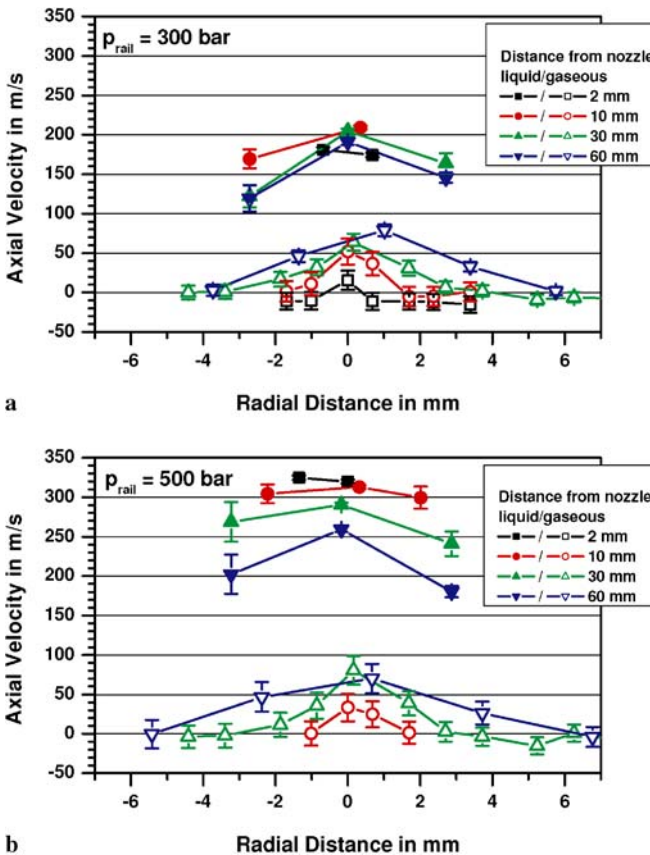


**FIGURE 4** Axial velocity of liquid and vapor phases under ambient conditions with tracers  $\text{Eu}:(\text{FOD})_3$  and acetone;  $\Delta t_{abi} = 0.7$  ms, velocities from reduction of averaged images of 20 single shots. (a) Relative velocities at  $p_{\text{Rail}} = 300$  bar, (b) relative velocities at  $p_{\text{Rail}} = 500$  bar

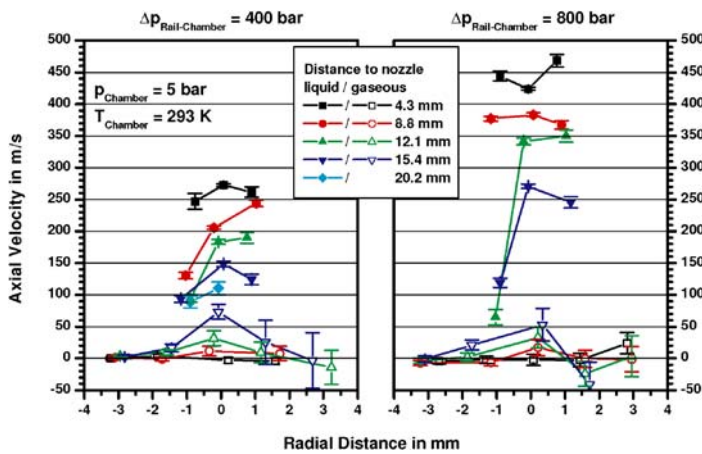


**FIGURE 5** Gas- and liquid-phase velocities at  $p_{\text{Chamber}}$  of 5 bar (reduction of averaged image of 50 laser pulses),  $\Delta p_{\text{Rail-Chamber}}$  of 400 bar and 800 bar with tracers acetone and  $\text{Eu}:(\text{FOD})_3$ ;  $t_{\text{abi}} = 0.7$  ms,  $\Delta t_{\text{id}} = 1.0$  ms

462 m/s. At the timing of 0.7 ms after the beginning of injection and an injection duration of 1.0 ms, the droplet velocity at the higher rail pressure equals 96% of Bernoulli's velocity, but is significantly lower in the case of 400 bar with only 83%. As shown in the figure, droplet velocities are decreasing with increasing radial distance from the center line of the spray. The higher density of the ambient gas of 5 bar results in significant deceleration of the droplets to 54% (400 bar) and 63% (800 bar) of the maximum velocity obtained at the nozzle exit within 11 mm.

The velocity distribution in the gaseous phase for the low pressure in Fig. 5 shows similar behavior as for the atmospheric conditions in Fig. 4. The gas is accelerated with increasing distance from the nozzle up to 73 m/s at 15.4 mm. This yields a relative velocity of droplets and gas phase of 55 m/s. Within the accuracy of measurement, both the radial velocity distribution up to a distance of 12.1 mm and the maximum velocity in the gas phase of 53 m/s at the injection pressure of 800 bar roughly match the results of the low-pressure case. The relative error in the ranges of 3% and 15% for the liquid-phase velocities is low compared to the uncertainty in the gas phase. Here a minimum error of 15% is achieved on the center line at 15.4 mm, whereas it is sig-

nificantly higher at different positions and may exceed 50%.

The LFT technique for simultaneous velocimetry in both phases within the spray yields highest accuracy at low chamber pressure and moderate injection pressure. The overall measuring error for the relative velocity may be estimated to be a minimum of 21%.

#### 4 Conclusions

The first application of LFT to determine the gas-phase velocity in a dense automotive spray by the use of phosphorescent tracers like acetone and biacetyl is presented. Furthermore, seeding the atmosphere with acetone and the model fuel with a non-interfering soluble lanthanide-chelate complex like  $\text{Eu}:(\text{FOD})_3$  enables simultaneous velocimetry of droplets and the gas phase. This yields improved accuracy for the slip velocity, which is an important quantity that could not be measured in many ultra-dense sprays before.

The results yield highest measuring accuracy for the liquid velocity distribution in the ranges of 2% to 15% in the ultra-dense region of a diesel spray. Due to reduced signal-to-noise ratio and lower velocities, the measuring error is higher for the results in the gas phase, giving best accuracy in the dilute and less atomized region of the spray with

a relative error of about 15%. For both increasing distance from the center line and higher droplet density upstream towards the nozzle tip, the accuracy is reduced. Relative velocities can be determined with an error of at least 21% in this first approach.

**ACKNOWLEDGEMENTS** This work was funded by the Deutsche Forschungsgemeinschaft (DFG) under reference GR1336/8-1.

#### REFERENCES

- 1 L. Araneo, C. Tropea, Optimisation of PDA measurements in a diesel spray, in *Spray 99*, 1999
- 2 A. Cronhjort, Droplet velocities in a sliced diesel spray, in *Proc. 17th Annu. Conf. Liquid Atomization and Spray Systems (ILASS)*, 2001
- 3 H. Chaves, C. Kirmse, F. Obermeier, *Atomiz. Sprays* **14**, 589 (2004)
- 4 C. Schugger, U. Meingast, U. Renz, in *Proc. 16th Annu. Conf. Liquid Atomization and Spray Systems (ILASS)*, 2000
- 5 S. Hu, D.M. Mosbacher, J.A. Wehrmeyer, R.W. Pitz, in *40th Joint Propulsion Conf. Exhib.*, 2004, AIAA-2004-4167
- 6 N.M. Sijtsema, N.J. Dam, R.J.H. Klein-Douwel, J.J. ter Meulen, in *Aerospace Sciences Meet. Exhib.*, Reno, NV, 2001, AIAA-2001-0851
- 7 R. Miles, J. Grinstead, R. Kohl, G. Diskin, *Meas. Sci. Technol.* **11**, 1272 (2000)
- 8 B. Stier, M. Koochesfahani, *Exp. Fluids* **26**, 297 (1999)
- 9 C. Pauls, S. Wissel, G. Grünefeld, J. Deppe, in *ILASS Americas 18th Annu. Conf. Liquid Atomization and Spray Systems*, 2005
- 10 S. Krüger, G. Grünefeld, *Appl. Phys. B* **71**, 611 (2000)
- 11 C. Gendrich, M. Koochesfahani, D. Nocera, *Exp. Fluids* **23**, 361 (1997)
- 12 B. Hiller, R. Booman, C. Hassa, R. Hanson, *Rev. Sci. Instrum.* **55**, 1964 (1984)
- 13 H. Hu, M.M. Koochesfahani, *Exp. Fluids* **33**, 202 (2002)
- 14 H.W. Sidebottom, C.C. Badcock, J.G. Calvert, B.R. Rabe, E.K. Damon, *J. Am. Chem. Soc.* **94**, 13 (1972)
- 15 A. Lozano, B. Yip, R.K. Hanson, *Exp. Fluids* **13**, 369 (1992)
- 16 M. Staudt, U. Meingast, U. Renz, in *Proc. 2002 Fall Tech. Conf. ASME Internal Combustion Engine Division: Design, Application, Performance and Emissions of Modern Internal Combustion Engine Systems and Components* (ASME, New Orleans, Louisiana, USA, 2002), Vol. 39, p. 289
- 17 S. Ghosh, J.C.R. Hunt, *Proc. R. Soc. London Ser. A* **444**, 105 (1994)
- 18 C. Schulz, V. Sick, *Prog. Energ. Combust. Sci.* **31**, 75 (2005)
- 19 J. Chen, P.R. Selvin, *Bioconjugate Chem.* **10**, 311 (1999)